Research Paper

# SPOCK1/SIX1axis promotes breast cancer progression by activating AKT/mTOR signaling

**Ming Xu[1], Xianglan Zhang[2], Songnan Zhang[3], Junjie Piao[1], Yang Yang[1], Xinyue Wang[1], Zhenhua Lin[1]**

[1]Department of Pathology and Cancer Research Center, Yanbian University Medical College, Yanji, China
[2]Oral Cancer Research Institute, Yonsei University College of Dentistry, Seoul, South Korea
[3]Department of Oncology, Yanbian University Affiliated Hospital, Yanji, China

**Correspondence to:** Zhenhua Lin; **email:** zhlin720@ybu.edu.cn
**Keywords:** SPOCK1, SIX1, EMT, breast cancer, AKT/mTOR signaling pathway
**Received:** March 28, 2020 **Accepted:** September 28, 2020 **Published:** December 3, 2020



## ABSTRACT

**SPOCK1 is highly expressed in many types of cancer and has been recognized as a promoter of cancer progression. Its regulatory mechanism in breast cancer (BC) remains unclear. This study aimed to explore the precise function of SPOCK1 in BC progression and to identify the mechanism by which SPOCK1 is involved in cell proliferation and epithelial-mesenchymal transition (EMT). Immunohistochemistry (IHC) experiments and database analysis showed that high expression of SPOCK1 was positively associated with histological grade, lymph node metastasis (LN) and poor clinical prognosis in BC. A series of *in vitro* and *in vivo* assays elucidated that altering the SPOCK1 level led to distinct changes in BC cell proliferation and metastasis. Investigations of potential mechanisms revealed that SPOCK1 interacted with SIX1 to enhance cell proliferation, cell cycle progression and EMT by activating the AKT/mTOR pathway, whereas inhibition of the AKT/mTOR pathway or depletion of SIX1 reversed the effects of SPOCK1 overexpression. Furthermore, SPOCK1 and SIX1 were highly expressed in BC and might indicate poor prognoses. Altogether, the SPOCK1/SIX1 axis promoted BC progression by activating the AKT/mTOR pathway to accelerate cell proliferation and promote metastasis in BC, so the SPOCK1/SIX1 axis might be a promising clinical therapeutic target for preventing BC progression.**

## INTRODUCTION

Worldwide, breast cancer (BC) is the most frequently diagnosed and the most lethal gynecologic malignancy in women [1], and it is an increasing concern because of rising morbidity rates. Although major advances have been made in the treatment of BC, the prognosis for most patients would be significantly worse once metastasis occurs [2]. Metastasis is the impetus for most patient deaths and represents the fundamental challenge of clinical treatment for patients with BC. The initiation and metastasis of BC are intricate processes triggered by multiple genes and intracellular signal transduction cross-talk. Thus, looking for valid molecular hallmarks and understanding the mechanisms of BC initiation and metastasis processes are urgently needed.

Sparc/osteonectin, cwcv and kazal-like domains proteoglycan 1 (SPOCK1), is also known as TIC1, SPOCK, and TESTICAN, and it belongs to the multidomain testicular proteoglycan family [3]. This protein family includes SPARC, TESTICAN-2, and TESTICAN-3, which are associated with cell proliferation and metastasis [4]. SPARC has been properly reported in a variety of cancers [5, 6], emphasizing its involvement in cell proliferation, angiogenesis and epithelial-to-mesenchymal transition (EMT). Recent discoveries have revealed that SPOCK1

is overexpressed in colorectal cancer, non-small cell lung cancer and glioblastoma [7–9]. Meanwhile, some reports revealed that SPOCK1 may promote the invasion and metastasis of gastric cancer and glioma [10, 11] and may confer a poor prognosis in urothelial carcinoma [12]. Nevertheless, the underlying mechanisms and functions of SPOCK1-induced BC activities, including cancer development and metastasis processes, are far from clear. Here, we described the oncogenicity of SPOCK1 and clarified the molecular mechanism of SPOCK1 involved in BC evolution.

EMT initially occurs in embryogenesis, and it is a kind of reversible and rapid change in cell phenotype, which is defined as changes in the epithelial phenotype into mesenchymal features [13], including loss of contact inhibition ability, promoting cell motility and invasiveness [14]. It is noteworthy that SIX homeobox 1 (SIX1), also known as BOS3, TIP39, and DFNA23, an indispensable transcription factor of organogenesis [15], plays a fatal role in promoting the cell EMT process [16–18]. SIX1 expression is negligible in normal adult organs, and its aberrant expression may lead to carcinogenesis [19]. Recently, SIX1 was found to be involved in cellular proliferation, invasion and the Warburg effect [16, 20]. In BC, SIX1 is highly expressed in half of primary cancers and 90% of cancer metastases [21]. In addition, SIX1 contributed to the initiation and prognosis of tumors [22]. To date, there are no similar reports regarding the association between SIX1 and SPOCK1 in BC evolution.

Herein, we aimed to reveal that overexpression of SPOCK1/SIX1 was related to BC cell proliferation and metastasis and predicted poor prognosis in BC patients via bioinformatic analysis of available BC datasets and immunohistochemical (IHC) assays. Additionally, we demonstrated that SPOCK1/SIX1 activated the PI3K/AKT/mTOR pathway, consequently promoting BC cell proliferation, accelerating cell cycle progression, and triggering the cell EMT program and metastasis, which provides new targets for BC therapies.

## RESULTS

### SPOCK1 was abnormally and strongly expressed and associated with metastasis and poor prognosis in BC

SPOCK1 was highly expressed in various cancers, including prostate cancer, pancreatic cancer, lung cancer and breast cancer (Figure 1A). We analyzed SPOCK1 mRNA expression across different datasets [23–25] from the Oncomine database and found that SPOCK1 was more highly expressed in BC than in normal tissues (Figure 1B). The median rank of SPOCK1 in highly expressed genes of BC was 672.0 based on a meta-analysis across seven datasets for Oncomine algorithms ($P$=1.06E-11) (Figure 1C). Furthermore, the UALCAN database, which integrated TCGA samples, showed the same results (Figure 1D). UALCAN also showed mRNA expression of SPOCK1 in 33 kinds of cancers, in which several cancers, including breast cancer, exhibited increased SPOCK1 expression. In the HPA database, SPOCK1 protein expression was hardly detected in normal sections, but there were significantly higher levels in BC (Figure 1E).

To further confirm the expression pattern of SPOCK1 in BC, 80 BC tissues and 10 adjacent nontumor tissues were examined by IHC assay. IHC analysis showed that SPOCK1 was significantly more highly expressed in BC tissues than in adjacent nontumor tissues. The positive rate (93.8%; 75/80) and strongly positive rate (72.5%; 58/80) of SPOCK1 in BC were both significantly higher than in adjacent nontumor tissues (30.0%, 3/10 and 10%; 1/10) ($P$<0.001) (Figure 1F, Table 1), which confirmed that SPOCK1 was aberrantly upregulated in BC. Notably, aberrant SPOCK1 expression was associated with histological differentiation ($P$=0.011) and LN metastasis ($P$=0.026) but not with patient age or ER and PR status (Figure 1G, Table 2). Moreover, high SPOCK1 expression was markedly related to unfavorable outcomes in BC patients. We evaluated the relationship between the SPOCK1 expression level and OS, RFS, PPS and DMFS of patients with BC using the Kaplan-Meier plotter database. As shown in Figure 1H, high SPOCK1 expression resulted in shorter OS, RFS, PPS and DMFS in various datasets. Finally, the level of SPOCK1 was significantly higher in the high-risk group than in the low-risk group according to the SurvExpress database. In general, these results underscored that SPOCK1 was strongly expressed in BC and could serve as an outcome predictor in BCs.

### SPOCK1 accelerated cell cycle progression and promoted cell proliferation in BC

To verify the potential oncogenic activity of SPOCK1 in BC, we surveyed endogenous SPOCK1 expression in a series of BC cell lines and a normal immortalized mammary gland cell line by western blot. Among the 7 cell lines, the MCF7 and SKBR3 cell lines exhibited high SPOCK1 expression, and the MDA-MB-231 and HS 578T cell lines showed low expression (Figure 2A). To explore the potential biological function of SPOCK1, we chose MCF7 and SKBR3 cell lines for SPOCK1 knockdown and MDA-MB-231 and HS 578T cell lines for stable SPOCK1 overexpression. The level of SPOCK1 expression in stable infected cell lines was

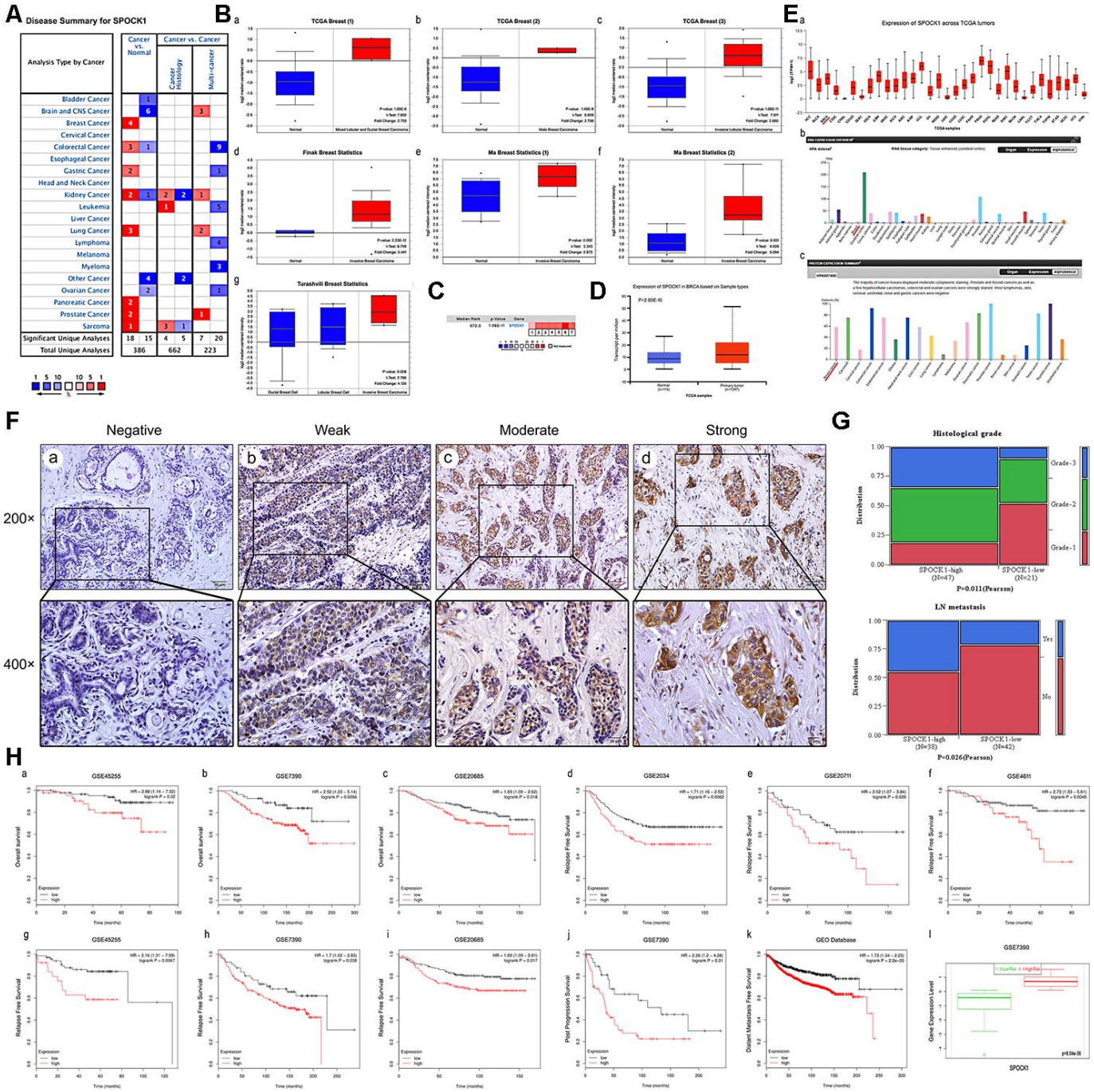


**Figure 1. Overexpression of SPOCK1 is positively associated with histological grade, LN metastasis and poor prognosis in BC.** (**A**) The graphic showed the numbers of datasets with statistically significant mRNA high expression (red) or down-expression (blue) of SPOCK1 (cancer vs. Normal tissue). The *P*-value threshold was 0.01. (**B**) Box plots derived from gene expression data in Oncomine comparing expression of SPOCK1 in normal and BC tissue. The *P*-value was set up at 0.01 and fold change was defined as 2. (**C**) A meta-analysis of SPOCK1 gene expression from seven Oncomine databases where colored squares indicated the median rank for SPOCK1 (vs. Normal tissue) across 7 analyses. (**D**) The expression of SPOCK1 was elevated in BC compared to normal breast tissues. Data derived from UALCAN database. (**E**) Expression of SPOCK1 across TCGA carcinomas from Ualcan database (a); overview of SPOCK1 protein levels in BC tissues and normal breast tissues (b-c). (**F**) IHC staining (negative, weak, moderate and strong expression) for SPOCK1 in BC tissues (a-d). (**G**) Relationships between SPOCK1 expression and clinicopathologically significant aspects of BC. (**H**) Overall survival (OS) (a-c), relapse free survival (RFS) (d-i), post progression survival (PPS) (**J**), distant metastasis free survival (DMFS) (k) and risk assessment curves (l) of patients with or without elevated SPOCK1 levels. Survival data derived from Kaplan–Meier (KM) plotter database. High SPOCK1 expression levels were found in high risk groups of BC patients. Box plots generated by SurvExpress showed the expression levels of SPOCK1 in indicated dataset and the *P*-value resulting from a *t*-test. Low-risk groups are denoted in green and high-risk groups in red, respectively.

**Table 1. SPOCK1 expression in BC.**

| Diagnosis | No. of case | Positive cases | | | | Positive rates | Strongly positive rates |
|---|---|---|---|---|---|---|---|
| | | - | + | ++ | +++ | | |
| **Breast cancer** | 80 | 5 | 17 | 26 | 32 | 93.8% | 72.5% |
| **Adjacent non-tumor** | 10 | 7 | 2 | 1 | 0 | 30.0% | 10.0% |
| $x^2$ | | | | | | 31.262 | 15.377 |
| ***P*** | | | | | | 0.000 | 0.000 |

**Table 2. Relationship between SPOCK1 expression and clinicopathologic features of BC patients.**

| Variables | No. of case | SPOCK1 strongly positive cases (%) | $\chi^2$ | *P* value |
|---|---|---|---|---|
| **Age** | | | | |
| ≥52 | 43 | 74.4%(32/43) | 0.172 | 0.679 |
| <52 | 37 | 70.3%(26/37) | | |
| **Histological grade** | | | | |
| Grade-1 | 20 | 45%(9/20) | | |
| Grade-2 | 30 | 73.3%(22/30) | 8.996 | 0.011* |
| Grade-3 | 18 | 88.9%(16/18) | | |
| **ER** | | | | |
| Positive | 50 | 70%(35/50) | 0.418 | 0.518 |
| Negative | 30 | 76.7%(23/30) | | |
| **PR** | | | | |
| Positive | 54 | 70.4%(38/54) | 0.653 | 0.419 |
| Negative | 24 | 79.2%(19/24) | | |
| **LN metastasis** | | | | |
| Yes | 26 | 65.4%(17/26) | 4.941 | 0.026* |
| No | 54 | 38.9%(21/54) | | |

*$P$<0.05 and **$P$<0.01

verified by western blot (Figure 2B), and the transfection efficiency is shown in Figure 2C. The best silencing effect was obtained with the shSPOCK1#2 and shSPOCK1#3 constructs for MCF7 and SKBR3 cell lines. Meanwhile, stable overexpression of SPOCK1 in MDA-MB-231 and HS 578T cells was exhibited.

MTT and EdU incorporation assays were used to determine the potential function of SPOCK1 in BC proliferation. As shown in Figure 2D, 2E, silencing SPOCK1 significantly suppressed cell growth, whereas SPOCK1 overexpression promoted cell proliferation. Similarly, upregulation of SPOCK1 facilitated cell clonogenicity, while SPOCK1 knockdown resulted in smaller and fewer colonies than the controls (Figure 2F). We further analyzed the influence of the cell cycle on SPOCK1 expression at different levels. The flow cytometry assay indicated that cells with higher SPOCK1 expression accelerated the progression of $G_2$/M phase, compared with the respective control (Figure 2G). Additionally, SPOCK1 knockdown decreased the levels of Cyclin-B1, CDK1, C-myc and Survivin, which was coupled with a concomitant increase in the expression of P21 and P27 (Figure 2H). Conversely, ectopic expression of SPOCK1 displayed harmful results. Together, the results demonstrated that SPOCK1 plays a crucial role in the BC cell cycle and proliferation *in vitro*.

*In vivo*, stable BC cells with modified SPOCK1 expression were subcutaneously injected into the fourth mammary fat pad of nude mice. The tumor volumes formed by cells with high SPOCK1 expression were significantly greater than those from cells with low SPOCK1 expression (Figure 2I). Additionally, the expression of Ki67 in the MCF7-NC group, SKBR3-NC group and MDA-MB-231-SPOCK1 group was much higher than it was in the negative control groups (Figure 2J). Overall, these findings suggested that SPOCK1 promoted BC cell growth *in vivo*.

**SPOCK1 promoted BC metastasis via the EMT process**

Next, we observed the metastatic ability of BC cells with different SPOCK1 expression. The wound-healing assay results indicated that cells with higher SPOCK1

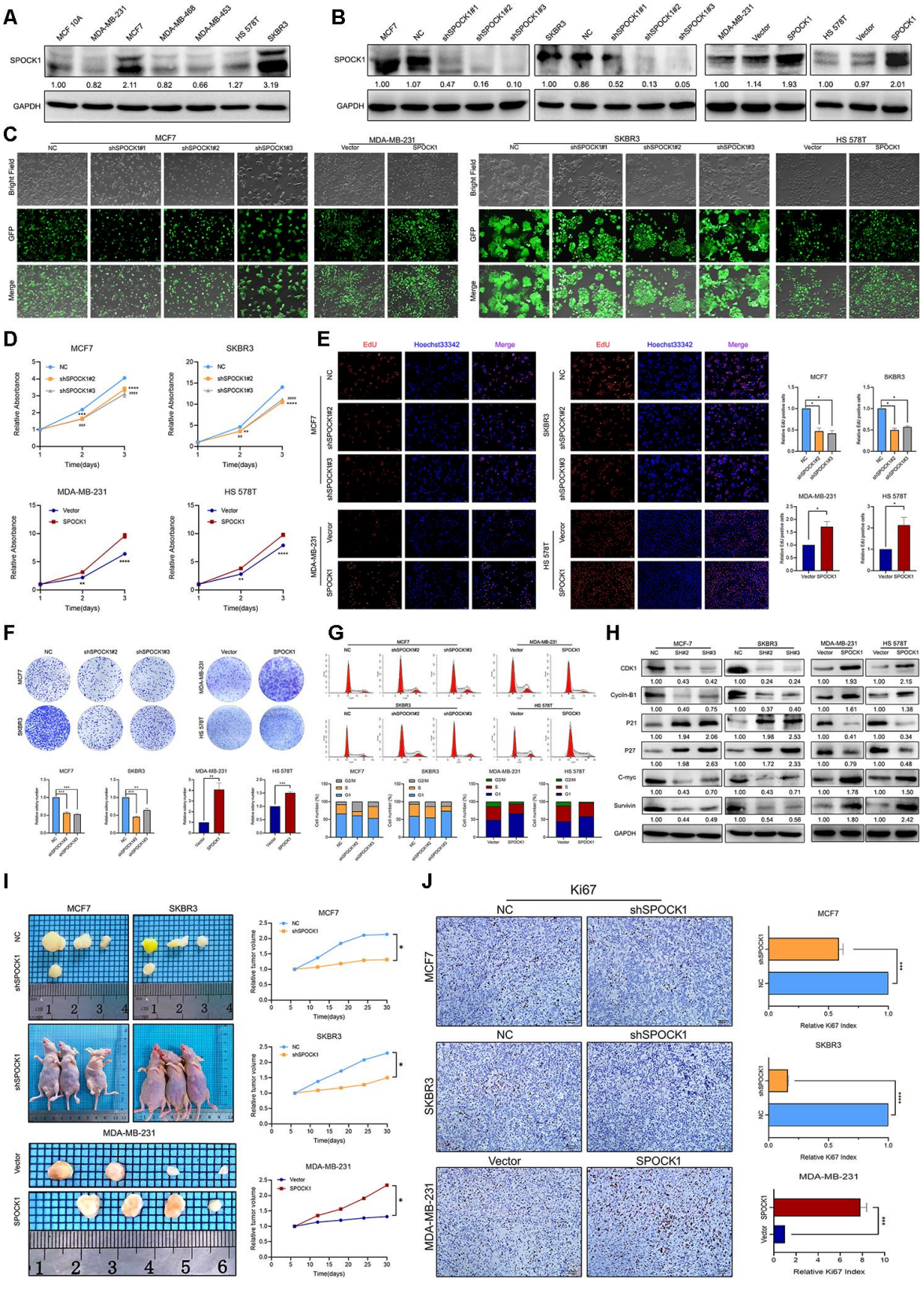

**Figure 2. SPOCK1 influences BC cell growth.** (**A**) Protein expression levels of SPOCK1 in BC cell lines as determined by western blot analysis. (**B**) MCF7/SKBR3 cells with SPOCK1 silencing and MDA-MB-231/HS 578T cells with SPOCK1 overexpression were established by viral transduction. The SPOCK1 levels in these established cell lines were verified by western blot analysis at 48 h after transfection. (**C**) Cells in bright light and GFP were captured to merge for displaying the transfection efficiency. (**D**) Cell viability was examined by MTT assay.

(**E**) Results of EdU assay on BC cells. Representative photographs are shown at the original magnification, ×100. (**F**) Cell clonogenic capacity was measured by colony formation assay. (**G**) Flow-cytometry analysis was performed to detect cell cycle progression. (**H**) The expression of proteins related cell cycle (CDK1, Cyclin-B1, P21, P27, C-mvc and Survivin) was determined by western blot analysis. GAPDH was used as a loading control. (**I**) Xenograft tumors formed by injecting the indicated cells. Relative tumor volume curves were summarized in the line chart (**P*<0.05). (**J**) IHC staining of the proliferation marker Ki67 in xenograft tumors. The relative percentage of Ki67-positive cells was summarized in the bar charts. The P values were obtained using t-tests (****P*<0.001, *****P*<0.0001). All results are from three independent experiments. The error bars represent the SD.

expression displayed a more widespread wound closure area than the corresponding control (Figure 3A). Transwell assays provided evidence that was consistent with those findings (Figure 3B). To further explore the effect of SPOCK1 on BC metastasis *in vivo*, stable cells with modified SPOCK1 expression were injected into the tail veins of nude mice. The number of pulmonary metastases in the higher SPOCK1 expression group was significantly greater than that in the corresponding control, which was opposite to the result in the lower SPOCK1 expression group (Figure 3C). Moreover, we found that the cells with higher SPOCK1 expression lost cell polarity, displayed spindle-shaped and acquired mesenchymal morphology with stronger invasion and metastasis ability, but lower SPOCK1 expression tended to have the opposite morphology (Figure 3D).

To determine whether EMT is responsible for SPOCK1-mediated changes in BC metastasis, we analyzed a cohort of 1101 BC samples from the TCGA dataset by the UCSC Cancer Genomics Browser. As presented in Figure 3E, we found that the heat maps of SPOCK1 in BC were strikingly coincident with VIM, SNAI2, TWIST1, and ZEB1 and inversely proportional to CDH1 (E-cadherin). Similarly, the GEPIA2 database also showed positive correlations between SPOCK1 and mesenchymal proteins (Figure 3F). Western blot and IF assays showed that downregulation of SPOCK1 accelerated the expression of epithelial markers and was accompanied by a reduction in mesenchymal markers (Figure 3G, 3H). Consistently, the group with high SPOCK1 expression displayed inverse results. Additionally, IHC staining results showed a higher expression of E-Cadherin and lower expression of Vimentin in shSPOCK1 group tumor tissue. Conversely, sections with high SPOCK1 expression displayed the opposite effects (Figure 3I). Taken together, these findings indicated that SPOCK1 enhanced EMT progression and triggered BC metastasis *in vitro* and *in vivo*.

**The oncogenic activity of SPOCK1 was significantly correlated with the AKT/mTOR pathway**

The AKT/mTOR signaling pathway has vital roles in cancer evolution, and its activation has been found in most BCs [26–29]. Thus, we speculated that SPOCK1 is involved in the regulation of the AKT/mTOR pathway in BC. Strikingly, depletion of SPOCK1 resulted in a decreased abundance of p-AKT, p-mTOR, p-S6 and p-4EBP1, where the total protein levels were not influenced (Figure 4A). Then, we further explored the role of the AKT/mTOR pathway in SPOCK1-mediated regulation of BC. We used the PI3K/AKT inhibitor LY 290042 and mTOR inhibitor rapamycin to block PI3K/AKT/mTOR activity and found that the inhibitors not only suppressed the activation of the PI3K/AKT/mTOR pathway but also reversed the promotion of SPOCK1 in the pathway. However, the inhibitors had no effects on SPOCK1 expression (Figure 4B). Indeed, LY290042 and rapamycin significantly suppressed the ability of SPOCK1 to accelerate BC cell proliferation and cell cycle progression (Figure 4C–4G). Similarly, inhibitors almost abolished the SPOCK1-mediated promotion of BC cell migration, invasion and EMT progression (Figure 4H–4J). These results demonstrated that SPOCK1 at least partly contributed to BC proliferation and EMT by activating the AKT/mTOR signaling pathway.

**SIX1 was aberrantly expressed and interacted with SPOCK1 in BC**

To further explore the molecular mechanisms underlying SPOCK1-induced BC proliferation and metastasis, we identified a potential target gene of SPOCK1 by bioinformatics strategies. We detected SPOCK1 protein-protein interactions by web-based databases, STRING and GeneMANIA, and intriguingly found that SPOCK1 was also associated with SIX1 (Figure 5A). The mechanism clarified that SIX1 could induce BC cells to undergo EMT progression and metastasis via the TGF-β pathway [30, 31]. Retrieval of the Oncomine database declared that SIX1 was highly expressed in breast cancer [23, 25] (Figure 5B–5E). The UALCAN and HPA databases showed the same results (Figure 5F). Moreover, HPA databases showed different positive staining intensities of SIX1 protein in BCs and negative staining in normal breast tissue (Figure 5G). Additionally, Kaplan Meier plotter and SurvExpress databases displayed that high levels of SIX1 expression resulted in poor OS, RFS and DMFS and acquired higher risk (Figure 5H). Overall, these data highlighted that SIX1 was highly expressed in BC and correlated with poor clinical outcome.

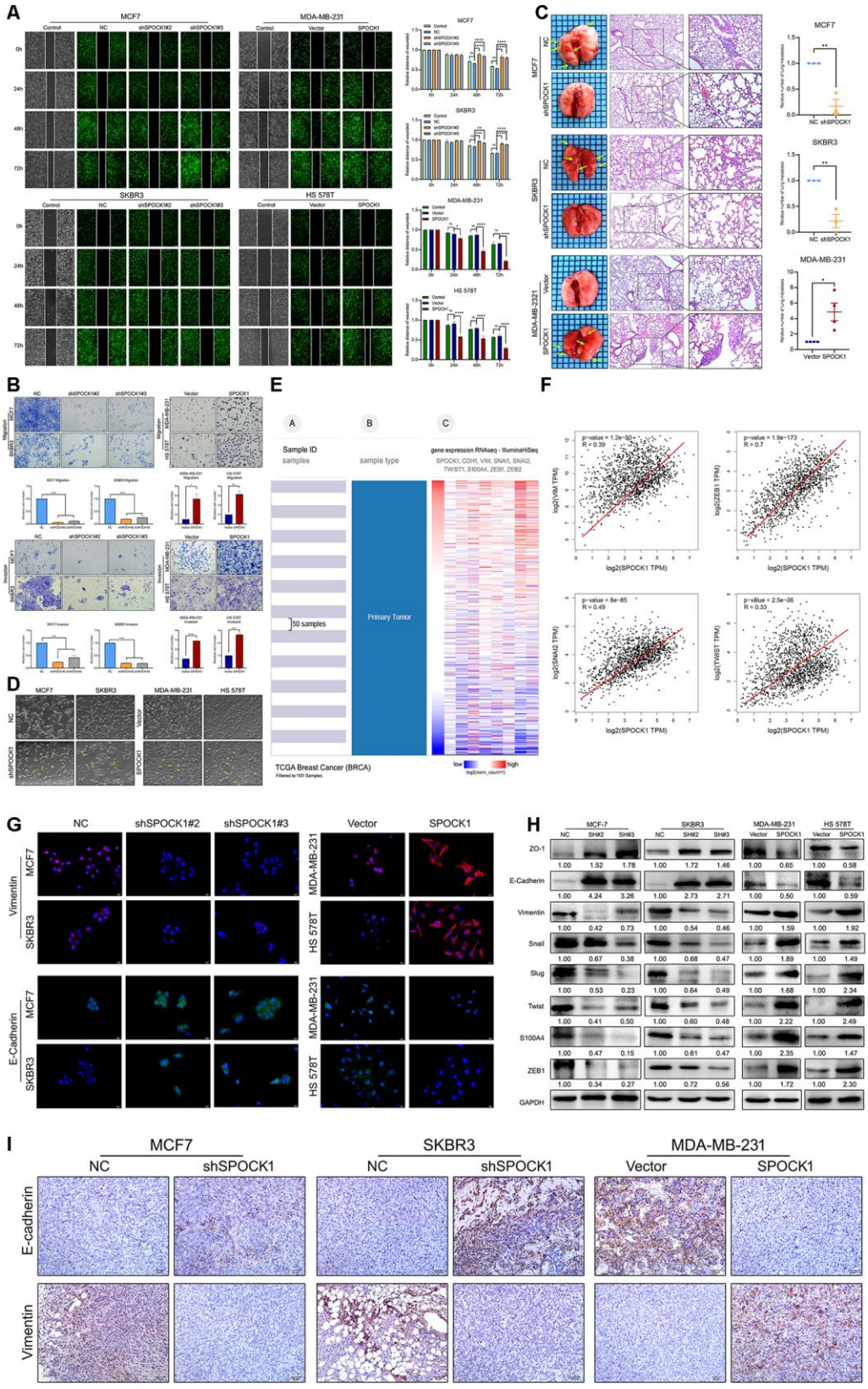


**Figure 3. SPOCK1 promotes cellular invasion, metastasis and the EMT *in vitro and in vivo*.** (**A**) A scratch wound-healing assay was used to determine the effects of SPOCK1 on BC cell motility. (**B**) Results of a transwell migration assay (a) and a Matrigel invasion assay (b) for cellular invasion. The mean number of cells in five fields per membrane is shown (×200). (**C**) Representative images of gross and hematoxylin and eosin (H&E) staining and relative numbers of lung surface metastatic foci detected in each group (*P<0.5, **P<0.01). The scale bar is 100

μM and 50 μM. (**D**) Representative images showing the morphological changes in the indicated cell lines. (**E**) The heat maps of the correlation between SPOCK1 and EMT markers in the same cohort. (**F**) Positive relationships for SPOCK1 and EMT markers were showed on GEPIA2. (**G**) The expression of EMT markers was detected by immunofluorescence staining in BC cells. The scale bar is 20 μM. (**H**) The expression of epithelial markers (E-cadherin and ZO-1) and mesenchymal markers (Vimentin, Snail, Slug, Twist, S100A4 and ZEB1) was determined by western blot analysis. GAPDH was used as a loading control. (**I**) IHC staining for E-cadherin and Vimentin protein in tumor specimens from xenografts (200×). The P values were obtained using Mann-Whitney U tests or t-tests (**P*<0.05, ***P*<0.01, ****P*<0.001, *****P*<0.0001). All results are from three independent experiments. The error bars represent the SD.

According to these data, we wondered whether SPOCK1 enrichment in cells was linked to SIX1. Consistent with our conjecture, IF and western blot assays showed that SIX1 was enriched in SPOCK1-highly expressed cells, whereas SPOCK1 knockdown decreased the level of SIX1 expression (Figure 5I, 5J). To further explore the potential binding interaction between SPOCK1 and SIX1, a coimmunoprecipitation (Co-IP) assay was performed. As shown in Figure 5K, we discovered the physical interaction of SPOCK1 with SIX1. Additionally, IF staining showed colocalization of SPOCK1 and SIX1 in the cytoplasm (Figure 5L). Taken together, our findings indicated that SIX1 interacted with SPOCK1 in BC.

### The SPOCK1/SIX1 axis regulated BC proliferation and metastasis via AKT/mTOR signaling activity

To explore the potential mechanism of SIX1 involved SPOCK1-induced proliferation, EMT and metastasis, we knocked down SIX1 expression in SPOCK1 stable overexpression cells by siRNA treatment (Figure 6A). As expected, silencing the expression of SIX1 effectively restrained SPOCK1-mediated cell proliferation, clone formation and cell cycle progression (Figure 6B–6E) and reversed SPOCK1-induced cell motility, migration and invasion (Figure 6F–6H). Furthermore, the downregulated expression of SIX1 substantially offset the SPOCK1-involved activation of AKT/mTOR signaling but did not affect the level of SPOCK1 expression (Figure 6I). Altogether, this evidence suggested that SIX1 silencing could, at least partially, abolish the biological behaviors that SPOCK1 induced in BC.

## DISCUSSION

SPOCK1 is a highly conserved extracellular matrix glycoprotein, with structural diversity and extensive tissue distribution that may be involved in multiple cell and extracellular matrix interactions [32]. A study has shown that SPOCK1 could enhance the expression and activity of MMP2 and MMP9, which can degrade extracellular matrix components and promote tumor cells to break through the cell barrier composed of the basement membrane and extracellular space matrix, thus causing tumor cells to migrate and invade surrounding tissues to distant tissues [11]. Additionally, SPOCK1 has been regarded as a candidate oncogene and have been verified to be closely related to the tumorigenesis, tumor progression, adhesion and metastasis of various tumors [33, 34]. Many biological phenomena have been observed in the function of the SPOCK1 gene, but the molecular biological mechanisms behind these phenomena are rarely studied.

Chen et al. reported that SPOCK1 was involved in slug-induced EMT and promoted cell invasion and metastasis, and high SPOCK1 expression was also reported to be a prognostic factor for poor survival in gastric cancer [10]. The results of this study documented that SPOCK1 was highly expressed in BC cells and clinical specimens relative to normal ones, which paralleled the Oncomine, HPA and Ualcan databases. IHC analysis showed that SPOCK1 was related to tumor histological differentiation and LN metastasis. Moreover, Kaplan Meier plotter database showed that BC patients with high SPOCK1 expression had poor OS, RFS, PPS and DMFS. Our findings were similar to the results in urothelial carcinoma (UC), in which higher SPOCK1 expression was correlated with unfavorable clinicopathological parameters and conferred a poor prognosis in UC [12]. Evidence from the SurvExpress database further showed that high expression of SPOCK1 had a higher risk in BC. These observations illustrated that SPOCK1 might play a crucial role in the treatment and prognosis evaluation of BC.

Infinite proliferation and metastasis are responsible for malignant tumor phenotypes, while initiation of EMT is the early step of the metastatic cascade. Unquestionably, EMT is identified as the dominant program in BC initiation and metastatic spread [35, 36]. A previous study revealed that deregulating the expression of SPOCK1 suppressed colorectal cancer (CRC) proliferation *in vitro* and *vivo*, and SPOCK1 was involved in CRC malignant features [7]. Notably, SPOCK1 was altered by EPCR to mediate 3D growth, consequently promoting breast cancer progression [37]. Here, we detected the variation in BC cells by modifying SPOCK1 expression, which revealed that SPOCK1 overexpression improved the proliferative and metastatic properties of BC cells and that suppression of SPOCK1 had the opposite effect. Xenograft and lung

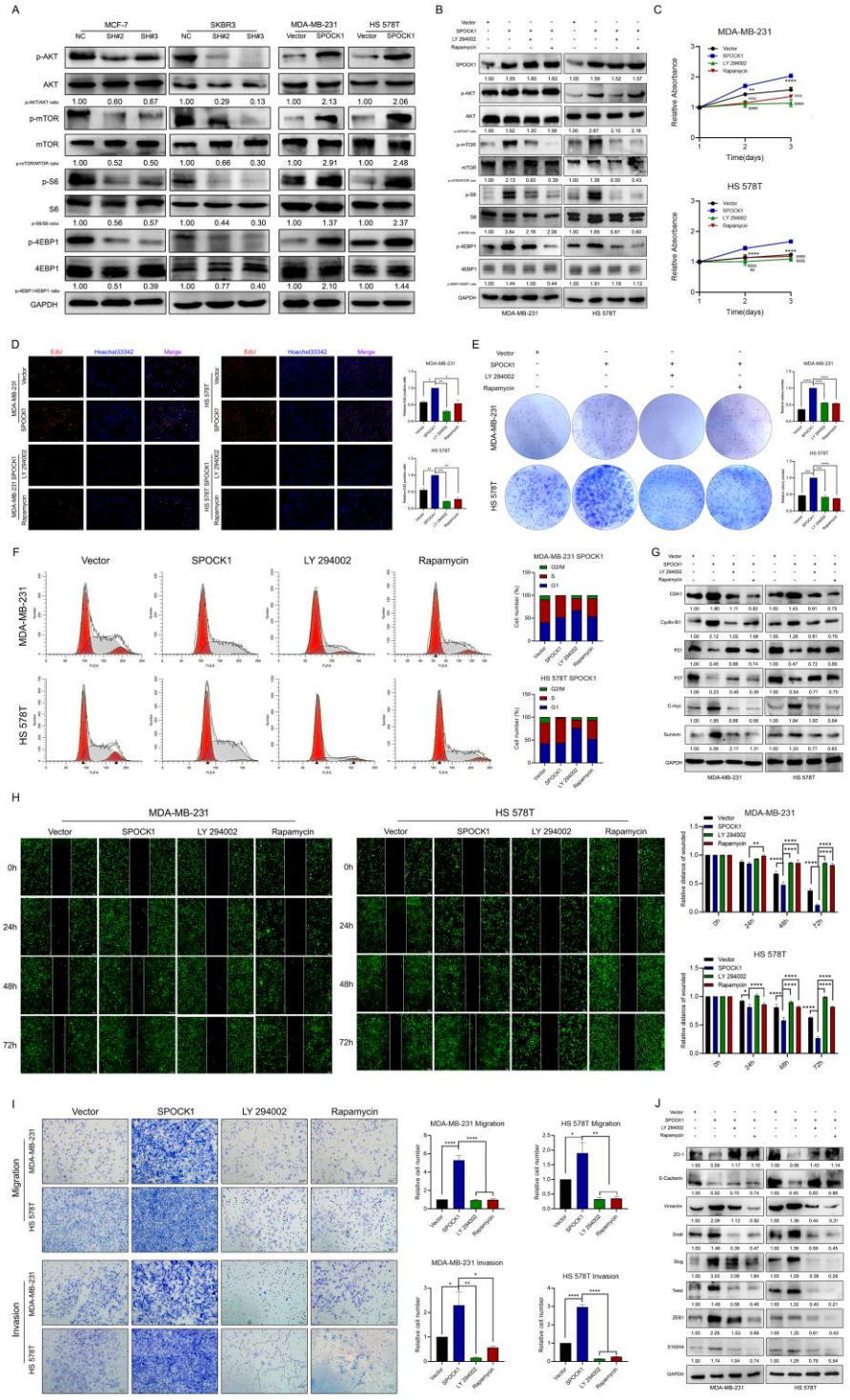

**Figure 4. SPOCK1 activates the AKT/mTOR signaling pathway in BC cells.** (**A**) Proteins level on AKT/mTOR pathway of indicated cells were assayed by western blotting. GAPDH was used as a loading control. (**B**) Stable BC cells were treated with LY 290042 or Rapamycin. Then indicated protein levels were assayed by western blotting. GAPDH was used as a loading control. (**C**–**E**) Cell viability was detected in SPOCK1-overexpressed cells after treatment with LY 290042 or Rapamycin by MTT assay (**C**), Edu staining (**D**) and colony formation (**E**) assays. (**F**) Cell cycle progression was assayed by flow-cytometry analysis after dealing with LY 290042 or Rapamycin. (**G**) Stable BC cells were treated with LY 290042 or Rapamycin. Then cell cycle related protein levels were assayed by western blotting. GAPDH was used as a loading control. (**H**–**I**) Cell motility and invasion capacities was detected in SPOCK1-overexpressed cells after treatment with rapamycin or LY294002. (**J**) Stable BC cells were treated with LY 290042 or Rapamycin. Then levels of EMT-related proteins were assayed by western blotting. GAPDH was used as a loading control. (*$P$<0.05, **$P$<0.01, ***$P$<0.001, ****$P$<0.0001).

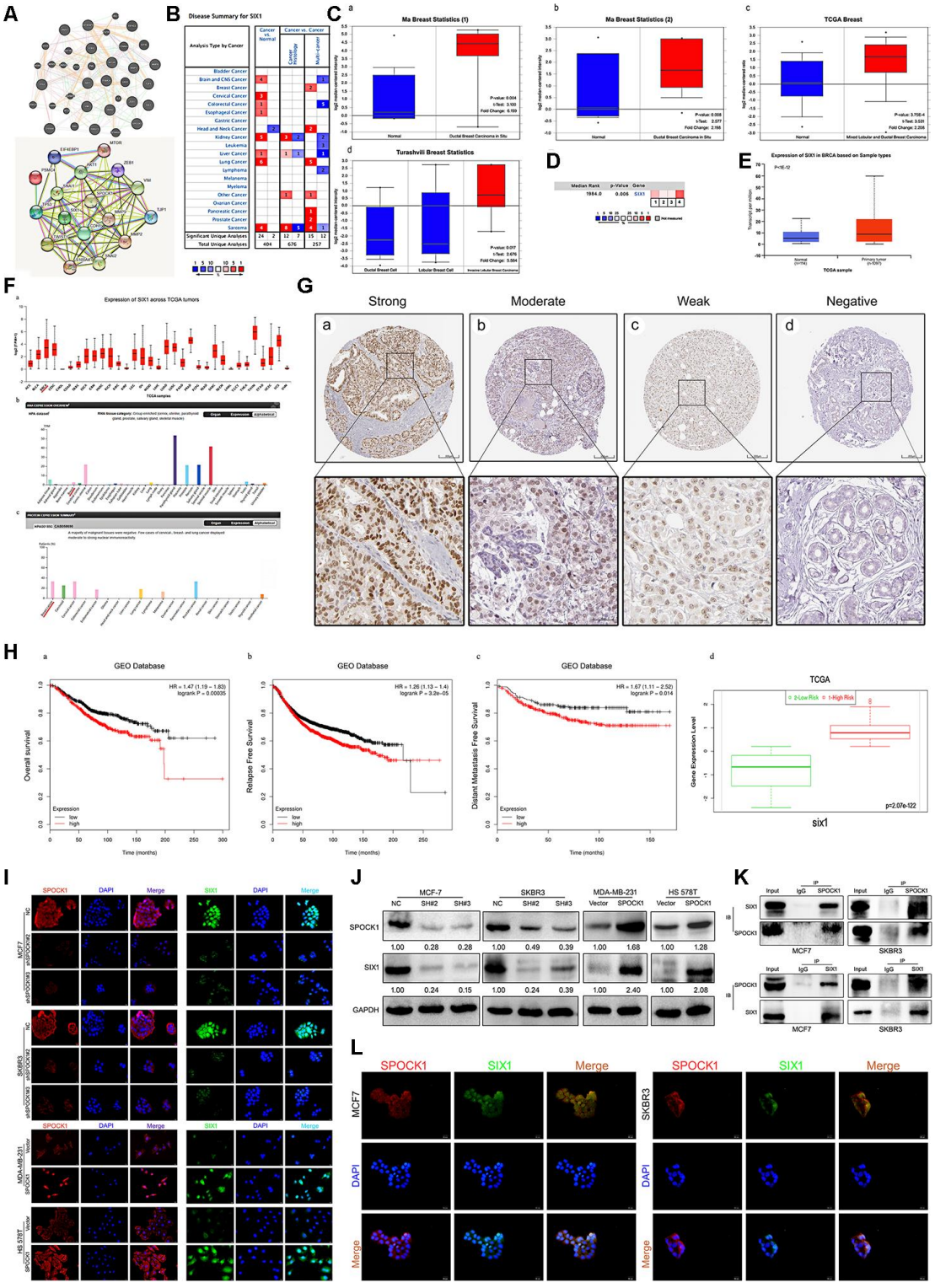


**Figure 5. Identification of SIX1 as a downstream mediator of SPOCK1 in BC cells.** (**A**) Network diagram of SPOCK1/SIX1 protein interaction by GeneMANIA (a) and STRING (b). (**B**) The graphic showed the numbers of datasets with statistically significant mRNA high expression (red) or down-expression (blue) of SIX1 (cancer vs. Normal tissue). The *P*-value threshold was 0.01. (**C**) Box plots derived from gene expression data in Oncomine comparing expression of SIX1 in normal and BC tissue. The p value was set up at 0.01 and fold change was defined as 2. (**D**) A meta-analysis of SIX1 gene expression from four Oncomine databases where colored squares indicated the median rank for SIX1 (vs. Normal tissue) across 4 analyses. (**E**) The expression of SIX1 was elevated in BC compared to normal breast tissues. Data derived from UALCAN database. (**F**) Expression of SIX1 across TCGA carcinomas from Ualcan database (a); overview of SIX1 protein levels in BC tissues and normal breast tissues (b-c). (**G**) IHC staining (negative, weak, moderate and strong expression) for SIX1 in BC tissues (a-d). Data derived

from HPA database. (**H**) Overall survival (OS) (a), relapse free survival (RFS) (b) and distant metastasis free survival (DMFS) (c) curves of patients with or without elevated SIX1 levels. Data derived from Kaplan–Meier (KM) plotter database. High SIX1 expression levels were found in high risk groups of BC patients (d). Data derived from SurvExpress database. (**I**, **J**) Expression levels of indicating cells were assayed by IF and western blotting. GAPDH was used as an internal control. (**K**) The interaction between endogenous SPOCK1 and SIX1 proteins was analyzed by coimmunoprecipitation in MCF7 and SKBR3 cells. (**L**) Immunofluorescence double-labeling experiments confirmed the existence of SPOCK1-SIX1 colocalization phenomena in the cytoplasm. The scale bar is 20 μM.

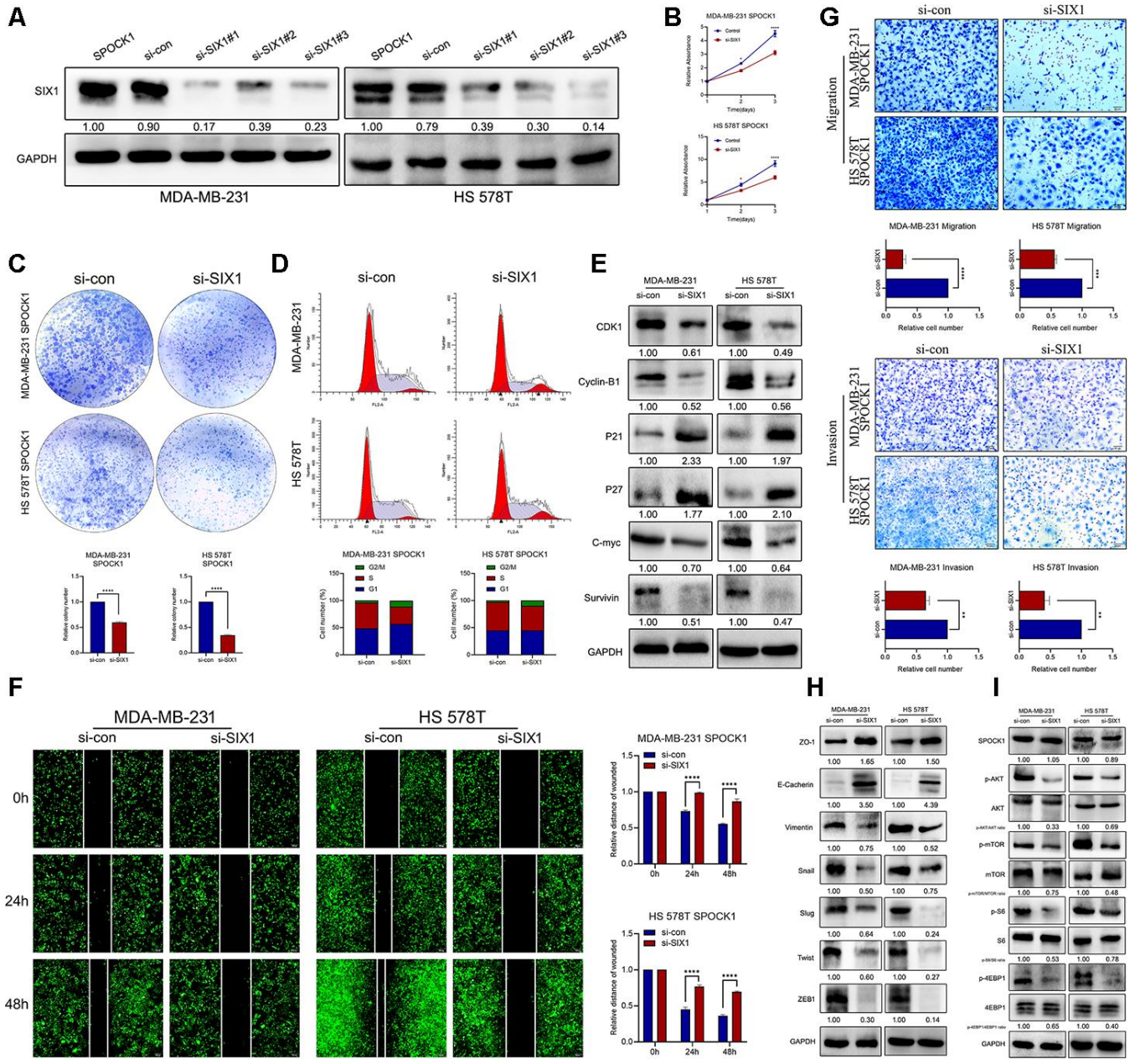


**Figure 6. SIX1 involved in SPOCK1-mediated BC progression.** (**A**) MDA-MB-231 and HS 578T cell line were transduced with si-con, si-SIX1#1, si-SIX1#2 and si-SIX1#3. The SIX1 levels in these were verified by western blot analysis after 48 h transfection. (**B**, **C**) Cell viability was detected in SPOCK1-overexpressed cells after transduction with si-RNAs by MTT assay (**B**) and colony formation (**C**) assay. (**D**) Cell cycle progression was assayed by flow-cytometry analysis after dealing with si-RNAs. (**E**) Stable BC cells were treated with si-RNAs. Then cell cycle related protein levels were assayed by western blotting. GAPDH was used as a loading control. (**F**, **G**) Cell motility and invasion capacities was detected in SPOCK1-overexpressed cells after treatment with si-RNAs. (**H**, **I**) Stable BC cells were treated with si-RNAs. The levels of EMT-related proteins and AKT/mTOR pathway were assayed by western blotting, respectively. GAPDH was used as a loading control. (**P*<0.05, ***P*<0.01, ****P*<0.001, *****P*<0.0001).

metastasis models further confirmed the *in vitro* results. Specifically, western blot and IF analyses showed that SPOCK1 increased the expression of mesenchymal markers and lost epithelial markers. Moreover, similar evidence was verified in xenograft mouse sections, suggesting that SPOCK1 triggered the EMT process both *in vitro* and *in vivo*.

The synthesis of multifarious signaling molecular events led to the oncogenesis of BC. Understanding and identifying these signaling mechanisms would restrain EMT progression to further therapeutically control cancer metastasis [38–40]. Previous studies reported that SPOCK1 could mediate EMT by the Wnt/β-catenin signaling pathway in non-small cell lung cancer [8], the PI3K/AKT signaling pathway in colorectal cancer, among other pathways [7]. Moreover, SPOCK1 blocked gallbladder cancer (GBC) cell apoptosis and promoted cell proliferation and metastasis by activating PI3K/Akt signaling both *in vitro* and *in vivo* [41]. In addition to AKT signaling, mTOR plays a crucial role in tumor proliferation and growth. Recent evidence has reported that the mTOR signaling pathway also plays a key role in tumor motility, invasion, and metastasis [42]. In renal carcinoma, activation of mTOR signaling promoted cell invasion ability by inducting EMT [43]. It has been verified that the mTOR inhibitor rapamycin could suppress cell scratch and chemotactic migration. In addition, the inhibition of mTOR decreased the formation of lamellipodia [44]. Consistent with this, pharmacologic and genetic inhibition of mTOR decreases colorectal cancer cell migration and invasion [45].

At present, targeting the PI3K/AKT/mTOR pathway as a therapeutic strategy to treat BC by is still an evolving field [46]. Thus, we were particularly interested in exploring the special role of SPOCK1 in the evolution of normal mammary glands to BC induced by the AKT/mTOR pathway. Our study revealed that SPOCK1 overexpression activates the AKT/mTOR pathway to promote the progression of BC. This was confirmed by the alterations of target proteins of the AKT/mTOR pathway, which was induced by depleting or overexpressing SPOCK1 expression and can be reversed by treatment with LY290042 or rapamycin, respectively. Furthermore, inhibition of the AKT/mTOR pathway by LY290042 or rapamycin treatment also impaired the effect of SPOCK1 upregulation on the cell cycle, proliferation and EMT process, verifying the effect of the AKT/mTOR pathway on SPOCK1-induced BC cell growth and metastasis.

SIX1 makes a notable contribution to tumor growth and metastasis [18, 47, 48]. SIX1 was identified to be involved in the oncogenic role of SPOCK1 in BC. Hyperactivation of SIX1 is widespread in a variety of human tumors and is associated with poor clinical efficacy. Emerging evidence has revealed that SIX1

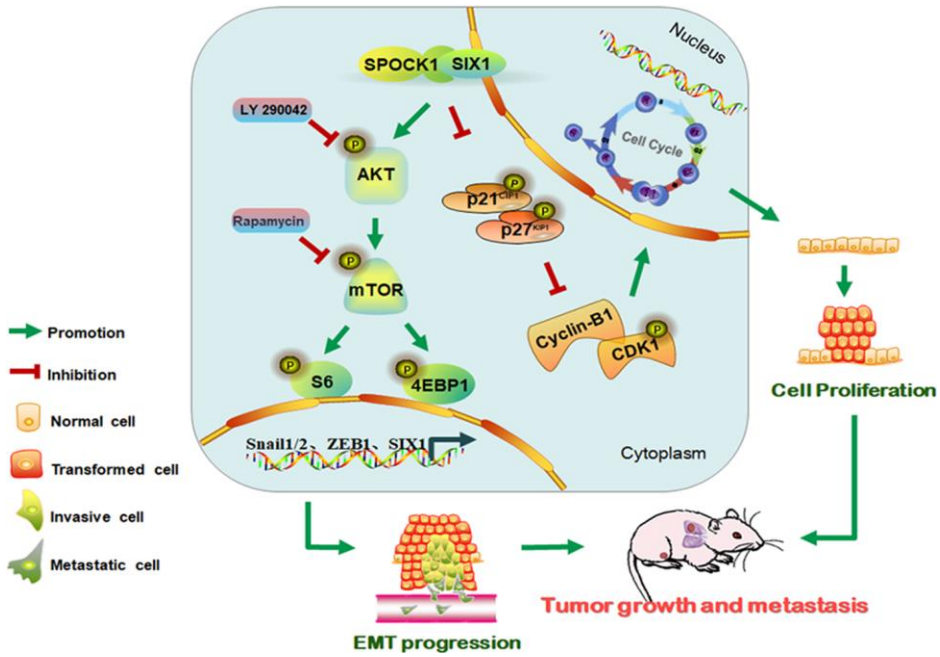


**Figure 7. Schematic of the proposed molecular mechanism of SPOCK1/SIX1 axis-induced BC cancer cell growth and metastasis.**

targets ERK and AKT signaling and promotes the malignant behavior of cancer cells [16, 49]. In accordance with this, we searched online databases and observed that SIX1 was frequently highly expressed in many cancers, including BC, and correlated with poor survival and high risk. Moreover, there was a statistically significant interaction between SPOCK1 and SIX1 that was identified by an online gene expression profiling interactive analysis tool. Based on these findings, we focused on the relationship between SPOCK1 and SIX1. As modified SPOCK1 expression led to significant changes in SIX1 levels, we then performed a Co-IP assay to confirm the interactive relationship. IF staining further showed that SPOCK1 and SIX1 were partly complexed together in the cytoplasm. Li et al. proposed that SIX1 participated in the transcriptional regulation of the Warburg effect in BC [20], providing critical evidence that SIX1 could act as a hallmark of cancer. Herein, to further identify the special role of SIX1 in SPOCK1-mediated BC evolution, we blocked the expression of SIX1 using siRNA and explored the effect on the cell cycle, proliferation, motility and EMT process. As we suspected, siSIX1 treatment significantly abolished SPOCK1-induced facilitation of BC progression without affecting the expression of SPOCK1 protein. Simply put, a large number of normative studies are still needed to clarify this molecular mechanism.

## CONCLUSIONS

In summary, this study contributed to illuminating the molecular mechanism by which SPOCK1 overexpression in human BC potentiated tumor progression. Our findings indicated that SPOCK1 is aberrantly overexpressed in BC. SPOCK1/SIX1 axis stimulated the AKT/mTOR signaling pathway to accelerate cell cycle progression, promote cell proliferation, trigger EMT progression and facilitate metastasis in BC (Figure 7). SPOCK1 along with SIX1 might be prognostic factors for BC patients and promising therapeutic targets involved in strategies to prevent BC progression.

## MATERIALS AND METHODS

### SPOCK1/SIX1 expression pattern

We performed SPOCK1/SIX1 mRNA expression in different cancers and confirmed the expression pattern of SPOCK1/SIX1 in BC by Oncomine database (https://www.oncomine.org/resource/login.html).

The comparison of different SPOCK1/SIX1 expression in various normal and cancer tissues and the expression of SIX1 protein in BC were used The Human Protein Atlas (HPA) (https://www.proteinatlas.org/) [50] and UALCAN (http://ualcan.path.uab.edu/analysis.html) [51] databases.

### Survival analysis

SPOCK1/SIX1 prognostic value in BC, including relapse free survival (RFS), distant metastasis free survival (DMFS), post progression survival (PPS) and overall survival (OS), was calculated by Kaplan-Meier plotter (http://kmplot.com/analysis/index.php?p=service&cancer=breast). Risk assessment was further assessed by SurvExpress (http://bioinformatica.mty.itesm.mx:8080/Biomatec/SurvivaX.jsp).

### Bioinformatics analysis

The protein and protein interaction networks in SPOCK1/SIX1 were established on the platform of GeneMANIA (http://genemania.org/) and Search Tool for the Retrieval of Interacting Genes (STRING) (https://string-db.org/cgi/input.pl) [52].

The heat map of the correlation between SPOCK1 and EMT markers in the same cohort was analyzed using UCSC Xena (http://xena.ucsc.edu/). The positive relationships for SPOCK1 and target genes were discerned and verified by Gene Expression Profiling Interactive Analysis 2 (GEPIA2) (http://gepia2.cancer-pku.cn/#index) [53].

### Cell culture

Human BC cell lines MCF7, MDA-MB-231, MDA-MB-453, MDA-MB-468, HS 578T, SKBR3 and normal immortalized mammary gland cell line MCF10A were cultured in Dulbecco Modified Essential Medium (DMEM) (Gibco, USA) with 10% FBS and 100 units penicillin and 100 mg/mL streptomycin.

### Plasmid construction and transfection

Human Lenti-shSPOCK1-GFP, Lenti-SPOCK1-GFP and negative control (Lenti-shNC and Lentivector control) were designed and packaged by Genechem (Co. Ltd., Shanghai, China). The target sequences of Lenti-shSPOCK1 were shown: 5'-TTTCGAGACGATGATTATT-3' for shSPOCK1#2 and 5'-GCTGGATGACCTAGAATAT-3' for shSPOCK1#3. The sequence of negative control was 5'-TTCTCCGAACGTGTCACGT-3'.

$2\times10^4$ BC cells were inoculated into 24-well plates for stable infection, then produce stably transfected cells by puromycin (2 μg/mL) after 48 h infection. The infection efficiency was identified by GFP gene reporter and western blot.

**Cell proliferation assay**

The 3-(4,5-dimethyl-2-thiazolyl)-2,5-diphenyl-2-H-tetrazolium bromide (MTT) assay was used to detect BC cell proliferation. Briefly, infected BC cells were seeded in plates and grown to 80% confluences for staining with MTT (0.5 mg/mL; 100 μL; Dako, Denmark) and dissolved the crystal by dimethylsulfoxide per 24 h for 5 d. Three wells per group at least were analyzed and repeated three times.

**Colony formation assay**

BC cells were inoculated in 6-well plates for incubating about 15 d. Then fixed the cells by methanol after being washed with cold PBS (Phosphate-buffered saline solution, Boster, China) and staining with Giemsa. Counting the colonies directly.

**5-ethynyl-2'-deoxyuridine (EdU) incorporation assay**

$5\times10^3$ BC cells seeded and grown in 96-well plates overnight and 100 μL 50 μM EdU medium (RiboBio, Guangzhou, China) per well were cultured for 2 h. Then the cells were fixed by methanol for 30 min and washing with PBS for 5 min twice. After permeabilizing with 0.5% TritonX-100 for 10 min twice and washing with PBS for 5 min, 1×Apollo dye was used to stain the cells for 30 min, repeated washing. Finally, the signal was visualized and recorded by a microscope after Hoechst 33342 counterstaining.

**Flow cytometry assay**

Washing the cells with 10 mL cold PBS, then centrifuging at 1000 rpm for 10 minutes and discarding the supernatant. Added 5 mL of 75% ethanol and incubated at -20° C overnight. Next day, washed twice with cold PBS to remove the ethanol, and centrifuged the cells for 10 minutes at 1500 rpm and discarded supernatant. Resuspension the cell pellets in 0.5 mL of PI/RNase Staining Buffer. After incubating 15 min at room temperature, stored tubes on ice freed from light prior to analyzing. Finally, samples were analyzed on the flow cytometer (BD Accuri C6) and used Modfit LT4.1 Software (Verity Software House, Inc., Topsham, ME, USA) to record the cell cycle distribution.

**Immunofluorescence (IF)**

BC cells were attached with 4% paraformaldehyde. Permeabilizing cells with 0.5% TritonX-100 for 15 min and blocking with 3% Albumin Bovine V (Solarbio, Beijing, China) for 2 h. Then incubating primary antibodies overnight at 4° C. Incubating with second antibodies (A1108, Invitrogen, USA), and counterstaining by DAPI with an Antifade Mounting Medium (Beyotime, Shanghai, China) the next day. Finally, cover-slips signal was captured by the microscope.

**Wound healing assay**

BC cells were seeded and grown in 6-well plates at approximately 80% confluences, scratching the monolayer uniformly on the surface by 200 μL. The scratched areas were recorded by microscope at 0h, 24h, 48h, and 72h. The migration distances were measured by Image J software for analyzing.

**Migration and invasion assay**

$3\times10^4$ BC cells were inoculated onto the upper chambers with or without coating Matrigel (BD Biosciences) containing 1% with serum in DMEM. Filling 20% fetal bovine serum/DMEM media into the lower chamber. The chambers were attached with 4% paraformaldehyde for 5 min after incubation for 24-48 h at 37° C, 5% $CO_2$. Then staining with Giemsa after washing with cold PBS. The migrated cells were counted by a microscope. The experiment was performed three times to reduce the possible effects of biological variability.

**siRNA transfection**

The sequence of si-SIX1 was SIX1-siRNA: 5'-GGG AGAACACCGAAAACAA-3'. BC cells were transfected with SIX1 siRNAs or control siRNA using Lipofectamine™ 3000 Reagent (Invitrogen, USA) according to the manufacturer's instruction.

**Western blot**

BSA Protein Assay Kit (A8020-5, Roche, Basel, Switzerland) was applied to measure the protein concentration after lysing BC cells with RIPA buffer. The total protein was dissolved by SDS-PAGE loading buffer and transferred onto poly vinylidene fluoride (PVDF) membranes (Millipore, Billerica, MA, USA). The primary antibodies (Table 3) were incubated overnight at 4° C. Second day, the HRP-conjugated secondary antibodies (CST, Danvers, MA, USA) were incubating for an hour, then antibody-reactive bands were visualized via enhanced chemiluminescence (ECL) system (Millipore, USA) in an Imager.

**Co-immunoprecipitation (Co-IP)**

In brief, added lysis buffer and incubated on ice for 30 min after washing the cell pellet with cold PBS. Scraped cells and centrifuged about 5 min, 15000 rpm, then transfer supernatant to a new microcentrifuge. Preclear the Protein A/G PLUS-Agarose beads (Santa Cruz,

**Table 3. The information of antibodies.**

| Antibodies | Source company | Dilution ration |
|---|---|---|
| Anti-SPOCK1 | R&D Systems，USA | 1:1000 |
| Anti-GAPDH | Proteintech, Wuhan, China | 1:1000 |
| Anti-p21(CDNK1A) | Proteintech, Wuhan, China | 1:1000 |
| Anti-p27[Kip1] | Proteintech, Wuhan, China | 1:1000 |
| Anti-CDK1 | Proteintech, Wuhan, China | 1:1000 |
| Anti-Cyclin-B1 | Cell signaling Technology，USA | 1:1000 |
| Anti-Survivin | Cell signaling Technology，USA | 1:1000 |
| Anti-C-myc | Santa Cruz, Dallas, Texas, USA | 1:1000 |
| Anti-Slug | Elibscience, Wuhan, China | 1:1000 |
| Anti-E-cadherin | Elibscience, Wuhan, China | 1:10000 |
| Anti-Vimentin | Cell signaling Technology，USA | 1:1000 |
| Anti-Snail | Cell signaling Technology，USA | 1:1000 |
| Anti-ZO-1 | Cell signaling Technology，USA | 1:1000 |
| Anti-Twist | Abcam, USA | 1:500 |
| Anti-S100A4 | Abcam, USA | 1:1000 |
| Anti-ZEB1 | Proteintech, Wuhan, China | 1:1000 |
| Anti-SIX1 | Sigma，USA | 1:1000 |
| Anti-p-AKT | Cell signaling Technology，USA | 1:2000 |
| Anti-AKT | Cell signaling Technology，USA | 1:1000 |
| Anti-p-mTOR | Cell signaling Technology，USA | 1:1000 |
| Anti-mTOR | Cell signaling Technology，USA | 1:1000 |
| Anti-p-S6 | Cell signaling Technology，USA | 1:1000 |
| Anti-S6 | Cell signaling Technology，USA | 1:1000 |
| Anti-p-4EBP1 | Cell signaling Technology，USA | 1:1000 |
| Anti-4EBP1 | Cell signaling Technology，USA | 1:1000 |

USA) with cold PBS and pre-blocked with BSA (Bovine serum albumin fraction V, Solarbio, China) to reduce non-specific immunoglobulin binding. Pellet beads, control IgG and 200 μL cell lysate incubated at 4° C about 1 h, transfer supernatant to a fresh microcentrifuge tube on ice and added 5 μL primary antibody and incubate overnight at 4° C, after centrifugation at 6500 rpm for 1 min at 4° C. Cap tubes and incubated at 4° C on a rocker platform overnight. Collected immunoprecipitates by centrifugation at 2500 rpm for 1 min at 4° C. Aspirated and discarded supernatant carefully. Washed pellet 3 times with lysis buffer, each time repeating centrifugation step above. After final wash, carefully aspirated and discarded supernatant and resuspended pellet in 20 μL of 3× electrophoresis sample buffer. Boiled samples for 5 minutes and analyze 25 μL aliquots by western blot.

**Mouse xenograft model**

To establish the orthotopic BC model, MDA-MB-231 cells stably overexpressing SPOCK1 (MDA-MB-231-SPOCK1) and MCF7 and SKBR3 cells stably silenced SPOCK1 (MCF7-shSPOCK1; SKBR3-shSPOCK1) as well as their negative control (MDA-MB-231-Vector; MCF7-NC; SKBR3-NC) were implanted in the mammary gland fat pad of BALB/c nude female mice (Viatal Rivers, Beijing, China). Injecting $10^6$ cells into the tail vein of 5-week-old nude mice for vivo lung metastasis models. Tumor sizes were monitored per 5 days, and volumes were calculated with a formula: Volume ($mm^3$) = 0.5 × length × width $^2$. About 5 weeks, all mice were sacrifices, then tumors and lungs were removed. The number of lung metastases was counted on the surface of the lungs. Finally, dissected tumors and lungs were hematoxylin and eosin staining.

**IHC staining analysis**

In brief, tissue sections were deparaffinized, rehydrated and incubated with 3% $H_2O_2$ for 15 min. Then performing in sodium citrate buffer (pH 6.0) at 95° C for antigen retrieval. After returning to the room

**Table 4. Immunohistochemical scoring according to immune-staining intensity and area.**

| Staining area(%) / Staining intensity | "0" (0-5%) | "1" (5%-25%) | "2" (25%-50%) | "3" (50%-75%) | "4" (75%-100%) |
|---|---|---|---|---|---|
| "0"(Negative) | Score0 | Score0 | Score0 | Score0 | Score0 |
| "1"(Week) | Score0 | Score1 | Score2 | Score3 | Score4 |
| "2"(Moderate) | Score0 | Score2 | Score4 | Score6 | Score8 |
| "3"(Strong) | Score0 | Score3 | Score6 | Score9 | Score12 |

temperature, the slides were incubated with primary antibodies overnight. Next day, secondary antibody was incubated for 2 h. The slides were developed in the reaction with a 3, 3'-diaminobenzidine chromogen and counterstained with Mayer's hematoxylin. Positive control and isotope control selected the tonsil and Rabbit IgG, respectively. Negative control treated positive tissue sections with PBS instead of primary antibody. Immunostaining for SPOCK1 was judged by a double semi-quantitative scoring system (Table 4). Specific reference to our previous research [54].

### Statistical analysis

Statistical analyses were carried out by SPSS version 17.0 software and Prism 8.0 for Windows. Chi-square tests ($\chi 2$) was used to compare the correlations between SPOCK1 expression and clinicopathological parameters. All data were displayed by mean ± standard deviation, which calculated for thrice experiments. One-way Anova was used to compare data between multiple groups, and pairwise comparisons between groups were performed by t-test. We considered $P<0.05$ as statistically significant.

### Ethics statement

Our study complied the Declaration of Helsinki and approved by the Human Ethics Committee and the Research Ethics Committees of Yanbian University in China. All patients signed informed consent, which included consent to use the resection specimens for scientific research. All the specimens were kept in our tissue specimen bank and we promised to provide privacy protection for patients.

Animal care and experimental procedures in this study were approved by the Institutional Animal Care and Use Committee (IACUC) of Changchun Weishi testing technology service co. LTD and performed in accordance with the institutional guidelines.

## AUTHOR CONTRIBUTIONS

Z. L. conceived this study and takes responsibility for the quality of the data. M. X., X. W. and Y. Y. participated in the experiments. S. Z. and Z. L. played an important role in interpreting the results. M. X. and J. P. performed the data analysis. M. X. wrote the manuscript and X. Z. helped to modify the manuscript. All authors read and approved the final manuscript.

## CONFLICTS OF INTEREST

The authors declare no conflicts of interest.

## FUNDING

This study was supported by grants from the Special Funds for Local Science and Technology Development Guided by the Central Committee, basic research project of Jilin Province (202002021JC), National Natural Science Funds of China (No. 31760313), The Funds of Tumen River Scholar Project and Key Laboratory of the Science and Technology Department of Jilin Province (No. 20170622007JC).

## REFERENCES

1. Siegel RL, Miller KD, Jemal A. Cancer statistics, 2020. CA Cancer J Clin. 2020; 70:7–30. https://doi.org/10.3322/caac.21590 PMID:31912902

2. Lee ES, Jung SY, Kim JY, Kim JJ, Yoo TK, Kim YG, Lee KS, Lee ES, Kim EK, Min JW, Han W, Noh DY, Moon HG. Identifying the potential long-term survivors among breast cancer patients with distant metastasis. Ann Oncol. 2016; 27:828–33. https://doi.org/10.1093/annonc/mdw036 PMID:26823524

3. Bradshaw AD, Sage EH. SPARC, a matricellular protein that functions in cellular differentiation and tissue response to injury. J Clin Invest. 2001; 107:1049–54. https://doi.org/10.1172/JCI12939 PMID:11342565

4. Li Y, Chen L, Chan TH, Liu M, Kong KL, Qiu JL, Li Y, Yuan YF, Guan XY. SPOCK1 is regulated by CHD1L and blocks apoptosis and promotes HCC cell invasiveness and metastasis in mice. Gastroenterology. 2013; 144:179–91.e4. https://doi.org/10.1053/j.gastro.2012.09.042 PMID:23022495

5. Naczki C, John B, Patel C, Lafferty A, Ghoneum A, Afify H, White M, Davis A, Jin G, Kridel S, Said N. SPARC inhibits metabolic plasticity in ovarian cancer. Cancers (Basel). 2018; 10:385. https://doi.org/10.3390/cancers10100385 PMID:30332737

6. Ma J, Gao S, Xie X, Sun E, Zhang M, Zhou Q, Lu C. SPARC inhibits breast cancer bone metastasis and may be a clinical therapeutic target. Oncol Lett. 2017; 14:5876–82. https://doi.org/10.3892/ol.2017.6925 PMID:29113221

7. Zhang J, Zhi X, Shi S, Tao R, Chen P, Sun S, Bian L, Xu Z, Ma L. SPOCK1 is up-regulated and promotes tumor growth via the PI3K/AKT signaling pathway in colorectal cancer. Biochem Biophys Res Commun. 2017; 482:870–76. https://doi.org/10.1016/j.bbrc.2016.11.126 PMID:27889608

8. Wang T, Liu X, Tian Q, Liang T, Chang P. Reduced SPOCK1 expression inhibits non-small cell lung cancer cell proliferation and migration through Wnt/β-catenin signaling. Eur Rev Med Pharmacol Sci. 2018; 22:637–44. https://doi.org/10.26355/eurrev_201802_14288 PMID:29461591

9. Yu F, Li G, Gao J, Sun Y, Liu P, Gao H, Li P, Lei T, Chen Y, Cheng Y, Zhai X, Sayari AJ, Huang H, Mu Q. SPOCK1 is upregulated in recurrent glioblastoma and contributes to metastasis and temozolomide resistance. Cell Prolif. 2016; 49:195–206. https://doi.org/10.1111/cpr.12241 PMID:26923184

10. Chen D, Zhou H, Liu G, Zhao Y, Cao G, Liu Q. SPOCK1 promotes the invasion and metastasis of gastric cancer through slug-induced epithelial-mesenchymal transition. J Cell Mol Med. 2018; 22:797–807. https://doi.org/10.1111/jcmm.13357 PMID:28940639

11. Yang J, Yang Q, Yu J, Li X, Yu S, Zhang X. SPOCK1 promotes the proliferation, migration and invasion of glioma cells through PI3K/AKT and Wnt/β-catenin signaling pathways. Oncol Rep. 2016; 35:3566–76. https://doi.org/10.3892/or.2016.4757 PMID:27108836

12. Ma LJ, Wu WJ, Wang YH, Wu TF, Liang PI, Chang IW, He HL, Li CF. SPOCK1 overexpression confers a poor prognosis in urothelial carcinoma. J Cancer. 2016; 7:467–76. https://doi.org/10.7150/jca.13625 PMID:26918061

13. Kalluri R, Weinberg RA. The basics of epithelial-mesenchymal transition. J Clin Invest. 2009; 119:1420–28. https://doi.org/10.1172/JCI39104 PMID:19487818

14. Elzamly S, Badri N, Padilla O, Dwivedi AK, Alvarado LA, Hamilton M, Diab N, Rock C, Elfar A, Teleb M, Sanchez L, Nahleh Z. Epithelial-Mesenchymal Transition Markers in Breast Cancer and Pathological Responseafter Neoadjuvant Chemotherapy. Breast Cancer (Auckl). 2018; 12:1178223418788074. https://doi.org/10.1177/1178223418788074 PMID:30083055

15. Ikeda K, Kageyama R, Suzuki Y, Kawakami K. Six1 is indispensable for production of functional progenitor cells during olfactory epithelial development. Int J Dev Biol. 2010; 54:1453–64. https://doi.org/10.1387/ijdb.093041ki PMID:21302255

16. Xie Y, Jin P, Sun X, Jiao T, Zhang Y, Li Y, Sun M. SIX1 is upregulated in gastric cancer and regulates proliferation and invasion by targeting the ERK pathway and promoting epithelial-mesenchymal transition. Cell Biochem Funct. 2018; 36:413–19. https://doi.org/10.1002/cbf.3361 PMID:30379332

17. Nishimura T, Tamaoki M, Komatsuzaki R, Oue N, Taniguchi H, Komatsu M, Aoyagi K, Minashi K, Chiwaki F, Shinohara H, Tachimori Y, Yasui W, Muto M, et al. SIX1 maintains tumor basal cells via transforming growth factor-β pathway and associates with poor prognosis in esophageal cancer. Cancer Sci. 2017; 108:216–25. https://doi.org/10.1111/cas.13135 PMID:27987372

18. Zhou H, Blevins MA, Hsu JY, Kong D, Galbraith MD, Goodspeed A, Culp-Hill R, Oliphant MUJ, Ramirez D, Zhang L, Trinidad-Pineiro J, Mathews Griner L, King R, et al. Identification of a Small-Molecule Inhibitor That Disrupts the SIX1/EYA2 Complex, EMT, and Metastasis. Cancer Res. 2020; 80:2689–2702. https://doi.org/10.1158/0008-5472.CAN-20-0435 PMID:32341035

19. Kumar JP. The sine oculis homeobox (SIX) family of transcription factors as regulators of development and disease. Cell Mol Life Sci. 2009; 66:565–83. https://doi.org/10.1007/s00018-008-8335-4 PMID:18989625

20. Li L, Liang Y, Kang L, Liu Y, Gao S, Chen S, Li Y, You W, Dong Q, Hong T, Yan Z, Jin S, Wang T, et al. Transcriptional regulation of the warburg effect in cancer by SIX1. Cancer Cell. 2018; 33:368–85.e7. https://doi.org/10.1016/j.ccell.2018.01.010 PMID:29455928

21. Ford HL, Kabingu EN, Bump EA, Mutter GL, Pardee AB. Abrogation of the G2 cell cycle checkpoint associated with overexpression of HSIX1: a possible mechanism of breast carcinogenesis. Proc Natl Acad Sci USA. 1998; 95:12608–13. https://doi.org/10.1073/pnas.95.21.12608 PMID:9770533

22. Kahlert C, Lerbs T, Pecqueux M, Herpel E, Hoffmeister M, Jansen L, Brenner H, Chang-Claude J, Bläker H, Kloor M, Roth W, Pilarsky C, Rahbari NN, et al. Overexpression of SIX1 is an independent prognostic marker in stage I-III colorectal cancer. Int J Cancer. 2015; 137:2104–13. https://doi.org/10.1002/ijc.29596 PMID:25951369

23. Turashvili G, Bouchal J, Baumforth K, Wei W, Dziechciarkova M, Ehrmann J, Klein J, Fridman E, Skarda J, Srovnal J, Hajduch M, Murray P, Kolar Z. Novel markers for differentiation of lobular and ductal invasive breast carcinomas by laser microdissection and microarray analysis. BMC Cancer. 2007; 7:55.

24. Finak G, Bertos N, Pepin F, Sadekova S, Souleimanova M, Zhao H, Chen H, Omeroglu G, Meterissian S, Omeroglu A, Hallett M, Park M. Stromal gene expression predicts clinical outcome in breast cancer. Nat Med. 2008; 14:518–27. https://doi.org/10.1038/nm1764 PMID:18438415

25. Ma XJ, Dahiya S, Richardson E, Erlander M, Sgroi DC. Gene expression profiling of the tumor microenvironment during breast cancer progression. Breast Cancer Res. 2009; 11:R7. https://doi.org/10.1186/bcr2222 PMID:19187537

26. Pascual J, Turner NC. Targeting the PI3-kinase pathway in triple-negative breast cancer. Ann Oncol. 2019; 30:1051–60. https://doi.org/10.1093/annonc/mdz133 PMID:31050709

27. Kilbas PO, Akcay IM, Doganay GD, Arisan ED. Bag-1 silencing enhanced chemotherapeutic drug-induced apoptosis in MCF-7 breast cancer cells affecting PI3K/Akt/mTOR and MAPK signaling pathways. Mol Biol Rep. 2019; 46:847–60. https://doi.org/10.1007/s11033-018-4540-x PMID:30661182

28. Corti F, Nichetti F, Raimondi A, Niger M, Prinzi N, Torchio M, Tamborini E, Perrone F, Pruneri G, Di Bartolomeo M, de Braud F, Pusceddu S. Targeting the PI3K/AKT/mTOR pathway in biliary tract cancers: a review of current evidences and future perspectives. Cancer Treat Rev. 2019; 72:45–55. https://doi.org/10.1016/j.ctrv.2018.11.001 PMID:30476750

29. Cheng Y, Pan Y, Pan Y, Wang O. MNX1-AS1 is a functional oncogene that induces EMT and activates the AKT/mTOR pathway and MNX1 in breast cancer. Cancer Manag Res. 2019; 11:803–12. https://doi.org/10.2147/CMAR.S188007 PMID:30697072

30. Micalizzi DS, Wang CA, Farabaugh SM, Schiemann WP, Ford HL. Homeoprotein Six1 increases TGF-beta type I receptor and converts TGF-beta signaling from suppressive to supportive for tumor growth. Cancer Res. 2010; 70:10371–80. https://doi.org/10.1158/0008-5472.CAN-10-1354 PMID:21056993

31. Micalizzi DS, Christensen KL, Jedlicka P, Coletta RD, Baron AE, Harrell JC, Horwitz KB, Billheimer D, Heichman KA, Welm AL, Schiemann WP, Ford HL. The Six1 homeoprotein induces human mammary carcinoma cells to undergo epithelial-mesenchymal transition and metastasis in mice through increasing TGF-beta signaling. J Clin Invest. 2009; 119:2678–90.

32. Iozzo RV, Murdoch AD. Proteoglycans of the extracellular environment: clues from the gene and protein side offer novel perspectives in molecular diversity and function. FASEB J. 1996; 10:598–614.

33. Wang Y, Wang W, Qiu E. SPOCK1 promotes the growth of osteosarcoma cells through mTOR-S6K signaling pathway. Biomed Pharmacother. 2017; 95:564–70. https://doi.org/10.1016/j.biopha.2017.08.116 PMID:28869894

34. Veenstra VL, Damhofer H, Waasdorp C, Steins A, Kocher HM, Medema JP, van Laarhoven HW, Bijlsma MF. Stromal SPOCK1 supports invasive pancreatic cancer growth. Mol Oncol. 2017; 11:1050–64. https://doi.org/10.1002/1878-0261.12073 PMID:28486750

35. Bill R, Christofori G. The relevance of EMT in breast cancer metastasis: correlation or causality? FEBS Lett. 2015; 589:1577–87. https://doi.org/10.1016/j.febslet.2015.05.002 PMID:25979173

36. Puisieux A, Brabletz T, Caramel J. Oncogenic roles of EMT-inducing transcription factors. Nat Cell Biol. 2014; 16:488–94. https://doi.org/10.1038/ncb2976 PMID:24875735

37. Perurena N, Zandueta C, Martínez-Canarias S, Moreno H, Vicent S, Almeida AS, Guruceaga E, Gomis RR, Santisteban M, Egeblad M, Hermida J, Lecanda F. EPCR promotes breast cancer progression by altering SPOCK1/testican 1-mediated 3D growth. J Hematol Oncol. 2017; 10:23. https://doi.org/10.1186/s13045-017-0399-x PMID:28103946

38. Li H, Batth IS, Qu X, Xu L, Song N, Wang R, Liu Y. IGF-IR signaling in epithelial to mesenchymal transition and targeting IGF-IR therapy: overview and new insights. Mol Cancer. 2017; 16:6. https://doi.org/10.1186/s12943-016-0576-5 PMID:28137302

39. Goswami MT, Reka AK, Kurapati H, Kaza V, Chen J, Standiford TJ, Keshamouni VG. Regulation of complement-dependent cytotoxicity by TGF-β-induced epithelial-mesenchymal transition. Oncogene. 2016; 35:1888–98. https://doi.org/10.1038/onc.2015.258 PMID:26148233

40. Ghahhari NM, Babashah S. Interplay between microRNAs and WNT/β-catenin signalling pathway regulates epithelial-mesenchymal transition in cancer. Eur J Cancer. 2015; 51:1638–49. https://doi.org/10.1016/j.ejca.2015.04.021 PMID:26025765

41. Shu YJ, Weng H, Ye YY, Hu YP, Bao RF, Cao Y, Wang XA, Zhang F, Xiang SS, Li HF, Wu XS, Li ML, Jiang L, et al. SPOCK1 as a potential cancer prognostic marker promotes the proliferation and metastasis of gallbladder cancer cells by activating the PI3K/AKT pathway. Mol Cancer. 2015; 14:12. https://doi.org/10.1186/s12943-014-0276-y PMID:25623055

42. Chen X, Cheng H, Pan T, Liu Y, Su Y, Ren C, Huang D, Zha X, Liang C. mTOR regulate EMT through RhoA and Rac1 pathway in prostate cancer. Mol Carcinog. 2015; 54:1086–95. https://doi.org/10.1002/mc.22177 PMID:25043657

43. Lamouille S, Connolly E, Smyth JW, Akhurst RJ, Derynck R. TGF-β-induced activation of mTOR complex 2 drives epithelial-mesenchymal transition and cell invasion. J Cell Sci. 2012; 125:1259–73. https://doi.org/10.1242/jcs.095299 PMID:22399812

44. Kwasnicki A, Jeevan D, Braun A, Murali R, Jhanwar-Uniyal M. Involvement of mTOR signaling pathways in regulating growth and dissemination of metastatic brain tumors via EMT. Anticancer Res. 2015; 35:689–96. PMID:25667447

45. Gulhati P, Bowen KA, Liu J, Stevens PD, Rychahou PG, Chen M, Lee EY, Weiss HL, O'Connor KL, Gao T, Evers BM. mTORC1 and mTORC2 regulate EMT, motility, and metastasis of colorectal cancer via RhoA and Rac1 signaling pathways. Cancer Res. 2011; 71:3246–56. https://doi.org/10.1158/0008-5472.CAN-10-4058 PMID:21430067

46. Costa RL, Han HS, Gradishar WJ. Targeting the PI3K/AKT/mTOR pathway in triple-negative breast cancer: a review. Breast Cancer Res Treat. 2018; 169:397–406. https://doi.org/10.1007/s10549-018-4697-y PMID:29417298

47. Xu H, Zhang Y, Peña MM, Pirisi L, Creek KE. Six1 promotes colorectal cancer growth and metastasis by stimulating angiogenesis and recruiting tumor-associated macrophages. Carcinogenesis. 2017; 38:281–292. https://doi.org/10.1093/carcin/bgw121 PMID:28199476

48. Wu W, Ren Z, Li P, Yu D, Chen J, Huang R, Liu H. Six1: a critical transcription factor in tumorigenesis. Int J Cancer. 2015; 136:1245–53. https://doi.org/10.1002/ijc.28755 PMID:24488862

49. Xin X, Li Y, Yang X. SIX1 is overexpressed in endometrial carcinoma and promotes the malignant behavior of cancer cells through ERK and AKT signaling. Oncol Lett. 2016; 12:3435–40. https://doi.org/10.3892/ol.2016.5098 PMID:27900017

50. Uhlén M, Fagerberg L, Hallström BM, Lindskog C, Oksvold P, Mardinoglu A, Sivertsson Å, Kampf C, Sjöstedt E, Asplund A, Olsson I, Edlund K, Lundberg E, et al. Proteomics. Tissue-based map of the human proteome. Science. 2015; 347:1260419. https://doi.org/10.1126/science.1260419 PMID:25613900

51. Chandrashekar DS, Bashel B, Balasubramanya SA, Creighton CJ, Ponce-Rodriguez I, Chakravarthi BV, Varambally S. UALCAN: a portal for facilitating tumor subgroup gene expression and survival analyses. Neoplasia. 2017; 19:649–58. https://doi.org/10.1016/j.neo.2017.05.002 PMID:28732212

52. Franceschini A, Szklarczyk D, Frankild S, Kuhn M, Simonovic M, Roth A, Lin J, Minguez P, Bork P, von Mering C, Jensen LJ. STRING v9.1: protein-protein interaction networks, with increased coverage and integration. Nucleic Acids Res. 2013; 41:D808–15. https://doi.org/10.1093/nar/gks1094 PMID:23203871

53. Tang Z, Kang B, Li C, Chen T, Zhang Z. GEPIA2: an enhanced web server for large-scale expression profiling and interactive analysis. Nucleic Acids Res. 2019; 47:W556–60. https://doi.org/10.1093/nar/gkz430 PMID:31114875

54. Xu M, Jin T, Chen L, Zhang X, Zhu G, Wang Q, Lin Z. Mortalin is a distinct bio-marker and prognostic factor in serous ovarian carcinoma. Gene. 2019; 696:63–71.